An Experimenter's Perspective on Validating Codes and Models with Experiments Having Shock-Accelerated Fluid Interfaces

Predictive science in the US Stockpile Stewardship Program requires precision experiments and analyses to validate physics models and fluid simulation codes.

In describing several science experiments used to validate applications of codes at Los Alamos National Laboratory, we offer an experimenter's perspective on this process within the context of the US Stockpile Stewardship Program. The validation of scientific code applications for simulating phenomena related to "weapons physics," the heart of the Stewardship Program, differs somewhat from traditional areas of physics.

The validation experiments[1–13] we describe validate particular models and algorithms that may be used in weapons codes. These validation experiments initially examined the physics well within the codes' domain of validity and thereby accumulated scientific evidence to assure that validity. More recently, experiments have matured sufficiently to investigate the boundary of code validity—for example, a limitation of a fluid simulation code is the smallest spatial scale at which a fluid instability can be resolved. Experiments are essential to determine the precise threshold spatial scale, meaning that the code can calculate instabilities accurately at larger scales, but not at smaller ones. Code resolution improvements can reduce the smallest resolvable spatial feature, but experimentation is the adjudicator to determine code accuracy. Our recent experimental work raises the standard of *validation science*[14,15] not only with experimental enhancements, but also with novel applications of analysis methods used to compare experimental data and simulation results.

Code validation at Los Alamos National Laboratory has changed with the cessation of underground nuclear weapons testing (UGT). During the UGT era, weapons codes—now called *legacy codes*—were used to design weapons, making the full-scale weapon test the ultimate validation experiment. The US is now committed to stewardship of the nuclear weapons stockpile without full-scale testing, so small-scale experiments validate code modules that are candidate improvements to weapons codes.

An essential module of a weapons code is fluid dynamics. This article discusses several experiments designed to validate the capability of a fluid simulation code—called a *hydrocode*—to calculate the complex flow of a fluid interface accelerated by a shock wave. This interaction is a fundamental phenomenon in the field of weapons physics.

The requirement of greater *predictive capability* in codes during an era of banned UGTs enhances the need for validation experiments focusing on the specific phenomena that may influence weapon

1521-9615/04/$20.00 © 2004 IEEE
Copublished by the IEEE CS and the AIP

Robert F. Benjamin
Los Alamos National Laboratory

performance. These experiments can focus on a physics model, such as a turbulence model, or on a combination of models and numerical methods, such as an adaptive mesh refinement (AMR) Eulerian calculation of a fluid instability that evolves into a disordered flow. Such experiments might be costly, large-scale, integrated, explosive experiments known as hydrotests; moderate-scale experiments requiring a multi-million-dollar facility, such as pulse power experiments;[16] or small-scale experiments conducted by one or two experimenters.

In this article, we describe a series of small-scale experiments conducted at a shock-tube facility at Los Alamos and how these shock-tube data have been used for model and code validation. Researchers have conducted similar small-scale experiments in the US, England, France, and Russia; for example, Jeffrey Jacobs' drop-tank experiments at the University of Arizona,[17] Malcolm Andrews' water-tank experiments at Texas A&M,[18] and Guy Dimonte's linear electric motor experiments at Lawrence Livermore National Laboratory.[19]

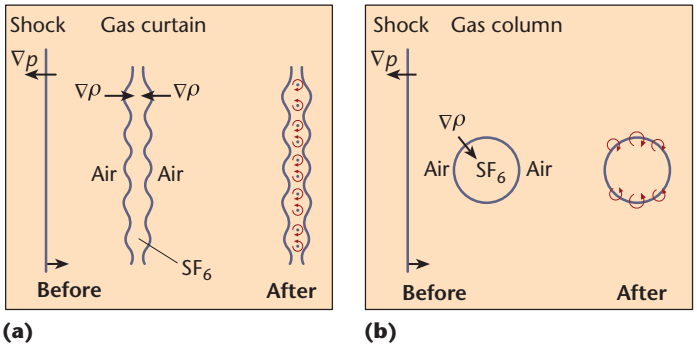

Figure 1. Shocked-gas experiments before and after shock-wave arrival, showing the pressure gradients (∇P) and density gradients ($\nabla\rho$). At the shock front, ∇P is directed opposite to the shock-wave velocity. (a) The density gradient for a gas curtain points into the SF_6 at both interfaces, and the RMI vorticity distribution is approximately a row of counter-rotating vortex pairs. (b) The density gradients for a gas cylinder point radially inward, and large vortices form where ∇P is nearly perpendicular to $\nabla\rho$.

The Physics of Shock-Accelerated Fluid Interfaces

A fluid interface subjected to acceleration is a fundamental problem in fluid dynamics as well as in weapons physics. A water surface subjected to gravity is a familiar example in fluid dynamics. The fluid interface is between water and the air above it; this interface is stable when air is above water ("stable" means that surface perturbations die away as damped gravity waves). However, when the interface is inverted so that the higher-density fluid (water) is above the lower-density fluid (air), the interface is unstable. The amplitude of a surface perturbation on a water-above-air interface grows exponentially with time and creates nonlinearities observed as a "spike and bubble" morphology. This phenomenon is called Rayleigh-Taylor instability (RTI), and it has become a classic problem for hydrocode validation.

If the acceleration at the interface is impulsive rather than constant, the phenomenon is Richtmyer-Meshkov instability (RMI), which occurs whether the acceleration is in the same or opposite direction as the density gradient ($\nabla\rho$) at the fluid interface. The physical basis for RMI, as well as RTI, is the baroclinic production of vorticity[20] shown in Figure 1. The misalignment of pressure gradient (∇P) and density gradients ($\nabla\rho$) at the interface produces vorticity, which causes instability growth manifest as the perturbation amplitude increases. The pressure gradient is caused by the shock wave or other impulsive acceleration in the RMI case and by gravity in the RTI case. RMI now refers to experiments like the gas curtain and gas cylinder, although earlier usage of it was restricted to the growth of initially small-amplitude perturbations (whereas initial perturbations in gas-curtain and gas-cylinder experiments are large). The initial distribution of air/SF_6 density gradients governs the post-shock vorticity distribution, as shown in Figure 1.

Experimental Facility and Diagnostics

The experimental facility shown in Figure 2 consists of a shock tube and the associated optical diagnostics. One or two experimenters can perform several dozen experiments daily. The shock tube is a six-meter-long hollow tube with a square cross-section inside, 75 × 75 mm. It comprises four sections: shock generator, driven section, experimental chamber, and runout. Just before the experiment, the shock generator is filled to high pressure with nitrogen gas. A solenoid-actuated knife ruptures a plastic diaphragm between the shock generator and driven section. This rupture initiates a shock wave that travels toward the experimental chamber at 400 m/sec (Mach 1.2 in air), and the shock wave becomes planar during its transit in the driven section. As the shock wave enters the experimental chamber, it first triggers several pressure transducers that measure the shock wave's speed and trigger the laser and cameras. Then it accelerates the sulfur hexafluoride (SF_6) gas target, a gas curtain or cylinder, described later. The shock wave continues into the runout section, where it reflects from the endwall. Optical measurements of the SF_6 target are complete before the reflected shock wave reacceler-

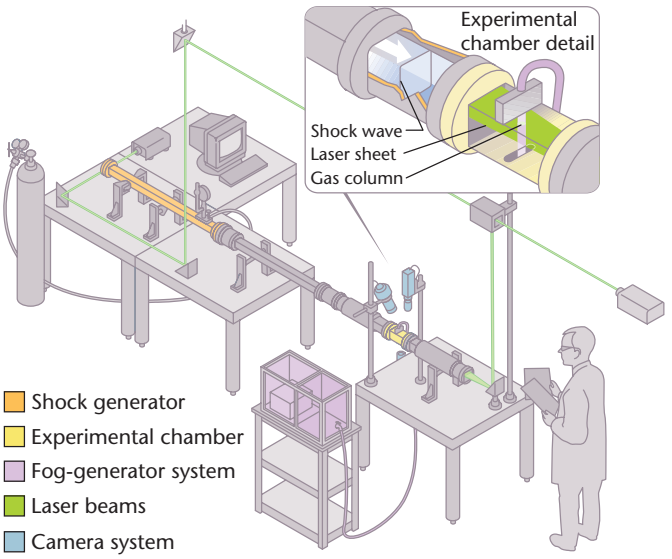

Figure 2. Experimental facility. A planar shock wave strikes a column of fog-traced sulfur hexafluoride (SF_6) gas formed in the air within the experimental chamber. Cross-sections of the column's density are photographed just before the shock wave arrives and at specific times later as the shock wave distorts the column.

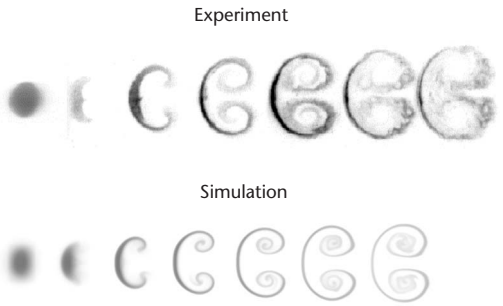

Figure 3. Experimental data versus computed simulation results for a shock-accelerated gas column. Darker regions are higher density. The snapshots at 140-μs intervals show the flow evolution, left to right, with the initial (pre-shock) condition at far left. Experiments and simulations show good agreement at larger spatial scales, while differences at smaller scales are being investigated further.

ates the target. Experiments can be performed with the endwall closer to the experimental chamber so that re-shock flows can be investigated. The sheet of pulsed laser light, 1-millimeter thick, enters the shock tube through a window in the endwall and illuminates a horizontal cross-section of the air/SF_6 flow; this cross-section image is recorded by a charge-coupled device (CCD) camera. The observation time is approximately 1 ms.

Early experiments used a gas curtain as the gas target, but later experiments used one or more cylinders of SF_6. Sample imaging data for the single-cylinder experiments are shown in Figure 3, in which all seven images were taken on the same experiment. These images are produced by laser light scattered from fog particles in the flow. The figure also shows a simulation of the experiment in which the SF_6 gas density forms the simulated image. The data and simulated images can be compared visually and quantitatively. The quantitative analyses include fractal dimension, histogram, and structure function.

To raise the standard of validation science, we supplement imaging data with 2D velocity field maps. We have used *particle-image velocimetry* (PIV) extensively to determine the 2D velocity fields in the plane illuminated by the laser sheet. Figure 4 presents a sample of velocity data. Our experience is that direct measurement of the velocity field in a complex flow tests a hydrocode's validity far more than mere imaging. The collaboration to compare experiment and simulation for the single-cylinder experiments with imaging and velocity fields[3] was far more challenging and useful for determining code limitations than was the earlier validation with gas-curtain experiments having only imaging data.[10]

PIV is a straightforward but difficult stroboscopic experimental technique whereby two images of a seeded flow are recorded with a small time interval—typically, a few microseconds in our experiments—and with sufficient spatial resolution to resolve the locations of tracer particles. The particle size, roughly 0.5 micron, is well below the camera resolution, but the particle location is well resolved. Using a correlation method, we obtain a 2D velocity vector of the flow for each cluster of 8 to 10 particles. Tracking individual particles requires seeding the flow with a much lower density of tracer particles, and the consequent spatial resolution associated with the velocity field would therefore be considerably lower. Consequently, we use a high seeding density and correlation-based analysis.

Gas-Curtain Experiments

During the summer of 1992, we began a series of gas-curtain experiments[5–13] in which the experimental chamber contained a slab or "curtain" of SF_6, about 3 mm thick, surrounded by air on both the upstream and downstream sides. A contoured nozzle shaped the cross-section of the slowly flowing SF_6. Because SF_6 is over five times denser than air, it easily falls through the air, and the flow's laminar character provides the distinct air/SF_6 boundary with the steep density gradient needed to excite RMI. For each series of experiments, a Mach 1.2 planar shock wave accelerated the gas curtain, and

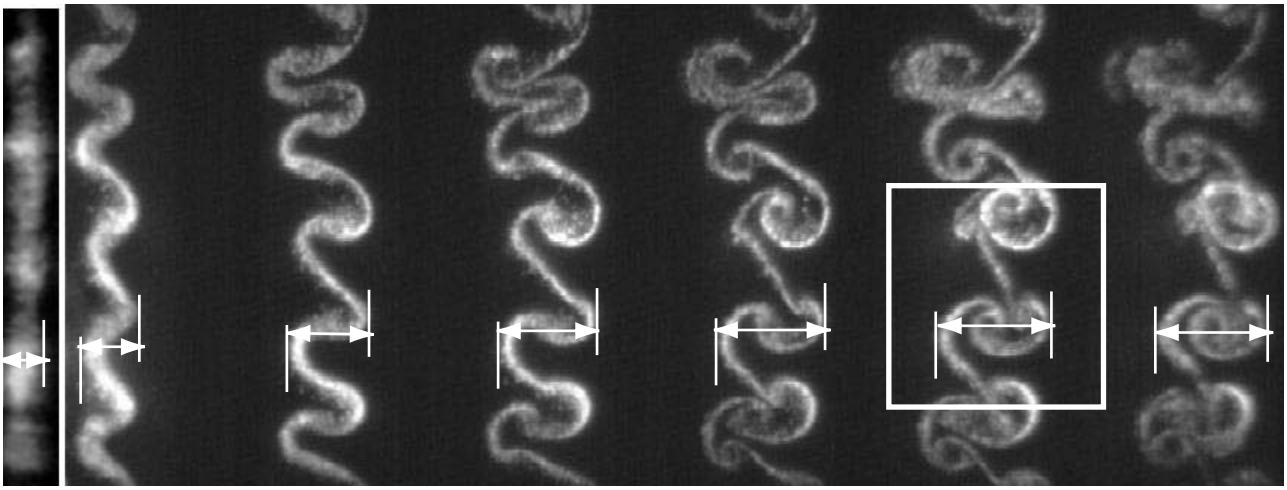

Figure 4. Sample velocity data. Initial conditions ($t = 0$) and dynamic images at $t = 115$, 255, 395, 535, 675, and 815 ms after shock interaction.

we developed progressively better diagnostics to measure the flow. For the first series, biacetyl vapor was mixed with the SF_6 gas to produce fluorescent images using planar laser-induced fluorescence.[12,13] Direct Rayleigh scattering from SF_6 molecules produced images during the second experimental series,[11] and scattering from tracer fog particles produced images during the third.[9] Thus, a succession of experimental diagnostics led to enhanced value of these experiments for code validation, and these experimental improvements led, in turn, to a better understanding of hydrocode limitations. We describe these enhancements in detail later.

Jacobs pioneered this experimental technique of creating the density gradient without using a thin membrane by using gas columns of SF_6 and helium.[21] He and others then used the laminar-flow method at Los Alamos to create the gas curtain.[12,13]

In the first series of gas-curtain experiments, we produced only one dynamic image per experiment and no image of the corresponding initial conditions. Consequently, these experimental results offered limited value for code validation because the calculations used idealized, not measured, initial conditions. Pat Crowley (Lawrence Livermore National Laboratory) did 2D calculations with idealized initial conditions and found that upstream–downstream asymmetry between perturbation amplitudes of the initial conditions could produce either upstream mushrooms or downstream mushrooms, depending on whether the initial upstream or downstream perturbations were greater, respectively. Rose Mary Baltrusaitis and her colleagues confirmed and quantified these effects.[10]

Although this first series of experiments was limited for use in code validation because the gas curtain's initial condition was not precisely measured on each event, they did identify three classes of post-shock flows: upstream-facing mushrooms, downstream-facing mushrooms, and sinuous patterns. These data stimulated the development of the Jacobs model to explain the growth of a row of counter-rotating, shock-induced vortices.[12] A vortex pair is the flow expected by RMI for a large-amplitude perturbation roughly sinusoidal in shape, and a mushroom image is the signature of a vortex pair. An important lesson is how the experimentation and modeling produced a boot-strapping effect when done collaboratively.[22] Exploratory experiments stimulated model development and, in turn, the model stimulated development of better diagnostics, leading to experiments that validated the model.

The second series of experiments produced two images per experiment, one of the initial condition just before the shock wave impacted the curtain, and the other of a dynamic image at a preset time after shock impact, typically several hundred microseconds. The images were created by Rayleigh scattering from SF_6 molecules; this scattering is less efficient than planar laser-induced fluorescence (PLIF). These data stimulated the validation of the Radiation Adaptive Grid Eulerian (RAGE) hydrocode,[23] and supported the development of mixed-cell and interface algorithms that dramatically improved the modeling of diffusive interfaces.[10] So, another important lesson is that validation experiments may precede the code maturation for doing the code validation.

The third series of experiments improved the flow's visualization so that many more images could

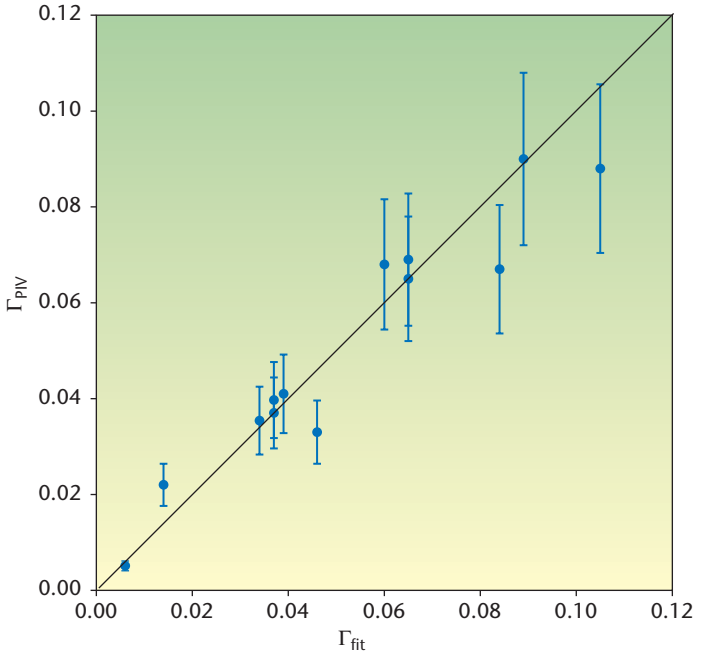

Figure 5. Validating the Jacobs model. Comparison of flow circulation measured using particle-image velocimetry (PIV) and estimated from the Jacobs model shows excellent agreement.

be recorded on each experiment. We seeded the SF_6 flow with a glycol-based tracer fog that scatters light far more efficiently than SF_6 molecules or biacetyl vapor. We could then observe as many as 30 images per experiment. However, to provide the best code-validation data, an experimental record of six dynamic images plus an initial-condition image optimized the trade-off between spatial resolution and number of images, as shown in Figure 4.

The successful fog-seeding technique led to an enhanced gas-curtain experiment by the application of velocity-field measurements via PIV. Gas-curtain experiments diagnosed with PIV enabled validation of the Jacobs model, as shown in Figure 5.

The key fitting parameter in the Jacobs model is the circulation (Γ_{fit}), the spatial integral of vorticity over each vortex. Jacobs proposed this model, based solely on density images, before we measured velocity fields. When we measured velocity fields with PIV, we could determine the circulation (Γ_{PIV}) from the velocity field data. Then we compared the measured values of circulation with those inferred from imaging data by analyzing the growth rate of vortices with the Jacobs model to determine the estimated, model-based circulation. As shown in Figure 5, comparing these two values for the circulation gave excellent agreement,[5] which validated the Jacobs model. This comparison demonstrates the predictive capability of the Jacobs model because it was formulated before explicit velocity-field measurements.

Single-Cylinder Experiments

Building on the code-validation success of gas-curtain experiments, we launched a series of single-cylinder experiments.[3] The conclusion of these experiments was that the RAGE code does well at calculating the bulk flow induced by baroclinic production of vorticity, but is limited in calculating the secondary shear instability that occurs during the onset of turbulence. The work leading to this conclusion provided many new challenges because this investigation was the first to use 2D velocity field data of a shock-induced flow to investigate code fidelity.

We studied velocity histograms as well as 2D maps of velocity and vorticity as shown in Figure 6. Comparisons between data and code output were complicated by ambiguities of reference frames and initial conditions. The experimenters and theorists expected the differences and worked hard to resolve them collaboratively. Consequently the ambiguities were resolved within experimental error for spatial scales ≥ 1 mm. However, the sub-mm vortices seen in experiments were not seen in calculations, presumably because of a Reynolds number effect. The experiment Reynolds number (ratio of inertial to viscous forces) is roughly 60,000, which is well above the laminar-to-turbulent transition, so codes designed for high-speed flows are expected to show these features. The presence of these micro-vortices provides one of the most detailed checks of the hydro algorithms in some codes.

Two essential lessons about code validation emerged from the single-cylinder code/experiment comparison. The first is the usefulness of the 2D velocity-field data in determining code limitations. If the only experimental diagnostic were multiframe imaging, not velocimetry, the comparison would have been far less sensitive. We would have observed the difference between code and experiment in the onset of the secondary instability at the leading edge of the vortex pair, but we would have failed to observe the secondary vortices associated with the shear instability. The second lesson is the value of iterating back and forth between calculation and experiment to elucidate the physics. When velocity magnitude spectra were not in agreement, for example, the calculation was improved by a better determination of the mean-flow velocity. When the calculation suggested that the initial density profile was more gradual than had been measured with fog seeding, the experiment was improved by imaging the initial conditions with direct Rayleigh scattering from SF_6 molecules, and this enhance-

ment showed the SF_6 diffusion in the initial cylinder that was not properly traced by the fog particles. Thus, we learned that successful code validation requires a collaborative, iterative approach in which both calculations and experiments can be improved to learn the code's capabilities and limitations. The result is confidence in both.

Double-Cylinder Experiments

Following the code-validation success of gas-curtain and single-cylinder experiments, we explored a more complex interaction between a planar shock wave and curved air/SF_6 interfaces. We changed the target from one to two cylinders aligned spanwise so that the shock wave impacted both of them simultaneously. This configuration complicates not only the shock wave/interface interaction, but also the subsequent flow's vortex dynamics—there are two interacting vortex pairs, rather than a single vortex pair. Our intuition proved to be correct, as the data showed three distinct flow morphologies that we labeled as *weak*, *moderate*, and *strong* interactions (see Figure 7). The strong interaction morphology consists of a single vortex pair, which was found to be a consequence of the initial condition where SF_6 diffusion reduced the modulation of density gradient in the region between the initial cylinders. The vorticity produced at the outer regions of each cylinder dominated the flow.

Comparisons between computations and experimental data showed significant differences on large, intermediate, and small scales when we used the initial conditions determined by fog-seeding as input for the calculation. We suspected that SF_6 diffusion during the cylinder formation rendered the air/SF_6 density gradients less steep than measured. However, calculations with estimated density gradients did not produce the experimental data. Mark Marr-Lyon's experimental images of initial conditions with direct Rayleigh scattering from SF_6 molecules quantified the error of fog-seeding in the initial condition, which was not predicted from calculation. When we used an SF_6 (non-fog) Rayleigh-scattered image for the calculations, the computed results matched the data at large and intermediate scales.

The agreement with the simulations was far from complete, however. For example, we observed small-scale features in the experimental vorticity field that were not seen in the computations. An experimental advance allowed us to quantify these differences. In the double-cylinder study, the experiment's repeatability was improved sufficiently to permit meaningful *ensemble averaging* for the first time in such a flow using a correlation-based tech-

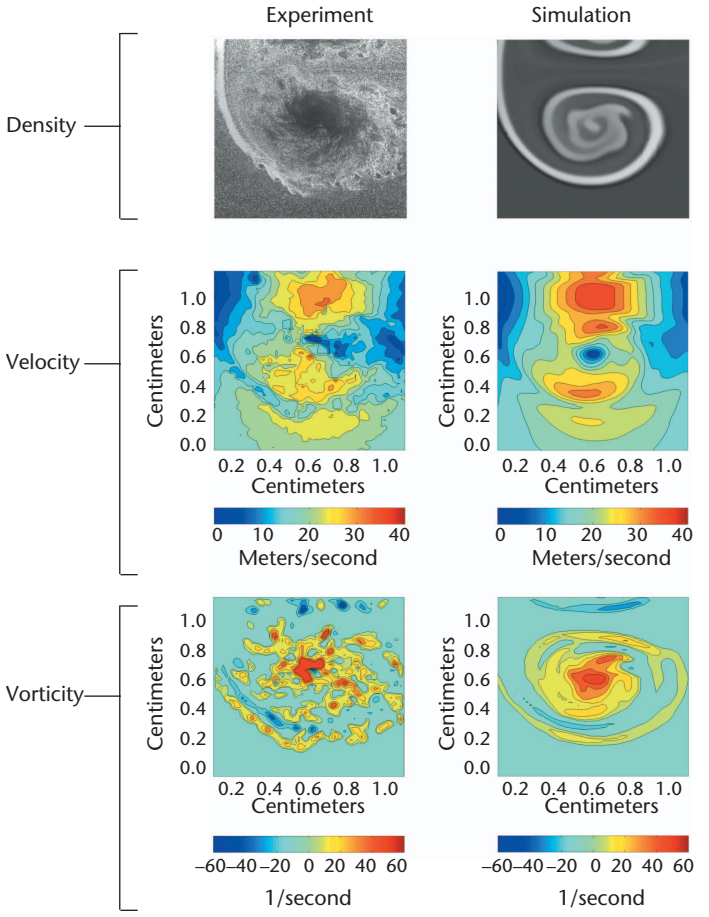

Figure 6. 2D maps of density, velocity and vorticity at 750 μs after shock/gas-column interaction, comparing experimental data versus computed simulation results. Vorticity signs and magnitudes, as well as large-scale density features, agree between experiment and simulation. However, significant differences exist at smaller spatial scales.

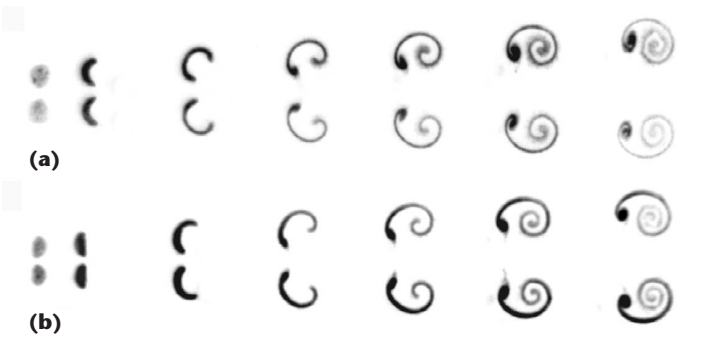

Figure 7. Flow morphologies. The two interacting, shock-accelerated gas cylinders are at moderate interaction, and the images are at t = 0, 50, 190, 330, 470, 610, and 750 μs after shock impact: (a) S/D = 1.6 and (b) S/D = 1.5. Images for experiments with larger initial separations show less asymmetry in each vortex pair and less rotation of the pairs relative to each other. For smaller initial separation, the images look similar to a single-cylinder result (see Figure 3).

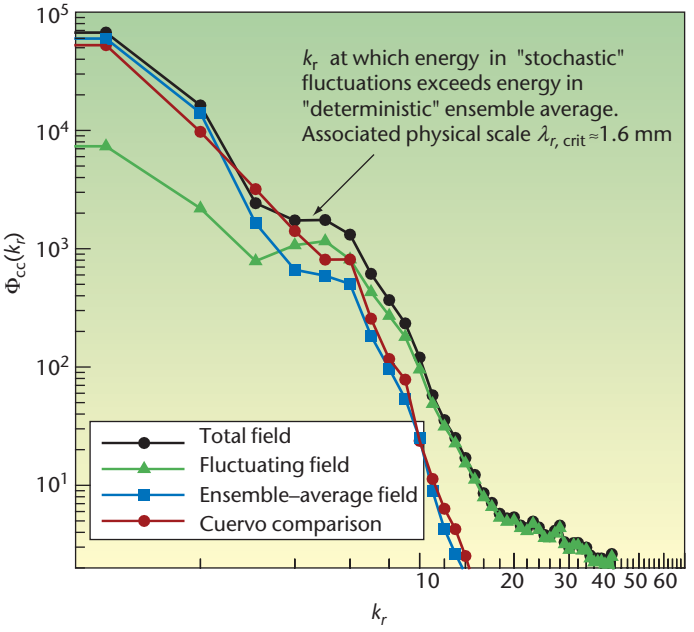

Figure 8. Simulation spectra. The various lines compare experimental data with the concentration power spectra for a Cuervo calculation that simulates the Navier-Stokes equations. The experimental concentration-field data are displayed in three components: the total field, the ensemble-averaged field, and the fluctuating field.

nique. We used the ensemble averaging method to decompose the concentration field into mean (deterministic) and fluctuating (stochastic) components. We calculated estimates of the concentration power spectra, assuming isotropy in the measurement plane, for the simulation and for the experiment's original, ensemble-average, and fluctuating fields. As shown in Figure 8, the simulation spectra agree with data for low wavenumber but show differences with the experimental results at higher wavenumber, where the small-scale features are manifest. The simulated results, however, showed excellent agreement with the spectra of the ensemble-average field—thus highlighting the agreement on the large and intermediate scales alone. This explicit demonstration of the relative lack of small-scale energy in the simulations provided strong motivation to move from 2D to 3D, which represents a significant advancement in William Rider's Cuervo code. The relative energy at different scales has recently been examined in the PIV data, and these data quantify the onset of turbulence.[1]

Progressive Validation

These highly resolved fluid-instability experiments are extremely useful for hydrocode validation because they exhibit complex and time-varying flow features. The interaction between the shock wave and initial interfaces also produces vorticity distributions that are complicated and sensitive to initial conditions. The flow becomes progressively disordered and eventually transitions into turbulence. However, soon after the shock/interface interaction, the flow appears ordered, so visual comparisons between experimental data and computational results, including overlay and differencing methods, are useful for "early-time" images.

Integral Methods

As the flow becomes disordered, integral metrics help us examine the large scales—an approach that is especially useful for model development. For example, the convention in studying RTI and RMI for a single interface is to plot a time history of the mixing zone width (MZW), which is the streamwise length scale that contains regions of both fluids. This scale is the sum of the bubble and spike heights for RTI. For RTI in the early times, the MZW grows exponentially, whereas it grows linearly for RMI. Various theories predict the time dependence of MZW at late times for these flows.

These integral metrics are valuable for the physical science of model development and provide some useful comparisons of code results with experiments. However, validation science demands more precise metrics of the disordered phase of these flows. Spectral methods provide a higher standard of comparing data and simulation results.

Spectral Methods

The application of structure-function analysis to gas-curtain data[8] and simulation[21] quantifies the visual perception that the "texture" of experimental and simulated images is substantially different during the disordered phase of the flow. The second-order structure function $S_2(l)$ is a measure of spatial autocorrelation as a function of l, a length scale that is the magnitude of the vector between two points in the image. For a given value of l, a large value of S_2 indicates strong autocorrelation in the image—for example, an image of a mesh would produce a large value of S_2 at the length scale equal to the mesh opening size and its multiples.

Using fog-seeded images of the gas curtain, James Kamm and his colleagues[24] found that two hydrocodes, RAGE and Cuervo, produced plots of S_2 versus l that agree well with each other (over nearly two orders of magnitude in l), but not with the experimental data, as shown in Figure 9. However, recent PLIF experiments with two- and three-cylinder targets suggest that this comparison might be limited by the fog seeding. This limita-

tion would be clarified by future applications of structure-function analysis to two- and three-cylinder PLIF data and their corresponding simulations, and/or by repeating the gas-curtain experiments with high-resolution PLIF measurements and repeating the simulations with appropriate initial conditions from experiments.

Fractal analysis is a spectral method that quantifies an image's boundaries and contours. In the case of an evolving fluid instability, the boundaries become contorted and complex. Fractal analysis provides a quantitative method to compare this growing complexity observed in the data and simulation results. The RAGE and Cuervo hydrocodes agree, but both disagree with experimental data for fog-seeded flows.

Analysis with a continuous wavelet transform (CWT) characterizes local behavior, in contrast to the more familiar Fourier transform that characterizes global or periodic properties of data. When applied to single-cylinder simulations and data, CWT shows a result analogous with fractal analysis—RAGE and Cuervo simulations agree well with each other, but not with experimental data.[2]

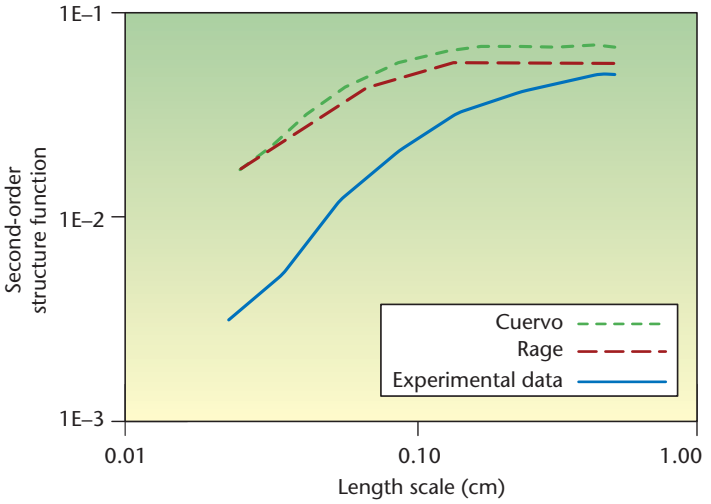

Figure 9. Cuervo versus RAGE. The different lines show second-order isotropic structure function versus length scale for the SF_6 fraction at 400 μs.

Velocity Fields

In addition to spectral methods for analyzing density or concentration images, validation science is elevated to a higher level in this project by the measurement and analysis of 2D velocity fields, which have been discussed for the gas-curtain and single-cylinder experiments. Our experience is that velocity fields provide a far greater challenge to codes than do density images.

Cultural Aspects of Code and Model Validation

Code and model validation can be done more effectively with contemporary experiments than with archival experiments because

- one can demonstrate predictive capability only with contemporary experiments, and
- the differences between data and theoretical/simulation results can be investigated better.

The parameter regime of contemporary experiments is limited and far from the operating conditions of nuclear explosives, so archival UGT and hydrotest data are essential. Each is necessary in the Stewardship Program.

Achieving a balance of these validations is problematic. On one hand, archival experiments produce "integrated physics" data, meaning that a measurement is the integrated result of a sequence of physics processes. Weapons designers can achieve a favorable comparison between simulation and data by adjusting different combinations of parameters corresponding to the sequence of processes. Determining which combination best approximates the actual physics of the component processes is difficult because the range of experiments is narrow and the physics is complex. On the other hand, "component physics" validation experiments, such as those discussed here for investigating fluid instability and the onset of turbulence, lead to better physics understanding and fewer adjustable parameters. Consequently, they produce more accurate algorithms, are more reliable for simulations that must extrapolate into new regimes, and demonstrate predictive capability. We observe that the Stewardship Program's culture appears to strongly favor the integrated physics validations, despite the mandate to enhance predictive capability.

Validation with contemporary experiments fosters close collaboration among experimenters, simulation researchers, analysts, and theorists. This collaboration creates a checks-and-balances dynamic based on the exploration of quantitative differences between experimental data and simulation results. The collaboration routinely exercises the scientific method whereby hypotheses are examined with experiments. The consequences are better validated codes and models as well as better experiments, which has certainly been the case for the shock-tube experiments presented here.

In contrast, validation with archival data often re-

veals inconclusively explained differences between experiment and simulation because no further experiments are possible. When experimental evidence for interpreting these differences is lacking, we often rely on expert judgment to make predictions and decisions. However, this judgment competes with validation science because it is based on experience and intuition, whereas validation science is based on data. Expert judgment is needed to make inferences about parameter regimes that cannot presently be accessed through validation science, but the risk of doing so is great. Despite this high risk, we observe that expert judgment is often misperceived as science, and that the stewardship culture lacks the systematic validation of the experts' credibility that was in place during the nuclear test era.

Because expert judgment is an important element of stewardship, the validation process is essential to ensure the experts' intuition and predictive capability. Accurate prediction of contemporary experimental data provides evidence of computationalists' acumen, and thereby attests to the reliability of their expert judgment and their comprehension of code limitations. Thus, proper validation of computationalists' credibility, in addition to that of models and codes, reduces the risk that expert judgment will make inaccurate predictions. In a high-stakes enterprise such as stockpile stewardship, the validation of researchers' judgment is a major benefit of contemporary validation experiments.

A difficulty of applying validation science is the structure of knowledge and ignorance in codes. Because we usually focus on knowledge and ignore how we manage our ignorance, weapons-physics computationalists are reluctant to apply the new understandings produced by contemporary experiments. Traditional physics disciplines (like nuclear and condensed-matter physics) localize ignorance in parameters such as "effective mass" and "effective potential" terms, so that improved experimental data can be efficiently applied to improve the physics models. In contrast, the complexity and history of nuclear explosives has led to the development of simulation codes in which ignorance is not localized, so the benefits of new code-validation data are far more difficult to accrue. Consequently, computationalists are reluctant to engage in validation exercises with contemporary experiments for fear of decalibrating codes by improving the physics models.

We observe an unfortunate, adversarial relationship[15] between researchers engaged in validation science with contemporary, collaborative experiments versus computationalists using only nuclear test data and hydrotests. This tension is apparent in the rhetoric—for example, simulation results for archival experiments are often called *data*, a term usually reserved for results of physical experiments; the code simulations are called *numerical experiments*. In contrast, researchers engaged in validation science with contemporary experiments use *data* to refer exclusively to experimental results and simulations or *calculations* to refer to codes, and they recognize clearly that the scientific method is the bedrock of science. We perceive this confusion of language as an effort to suggest that validation with archival data is more credible than it actually is, and we believe that such rhetoric problems complicate the process of validating codes for the Stewardship Program.

These fluid instability experiments will be modified to study turbulence and re-shock phenomena (that is, shock-accelerating the gas target a second time). Also, the diagnostics and data analyses developed for code validation will be applied to other experiments, such as interfaces driven by high explosives and radiographically diagnosed flows.

Acknowledgments

Postdoctoral researchers who have made outstanding contributions to this shock-tube project as part of their research careers include John Budzinski, Sanjay Kumar, Mark Marr-Lyon, Kathy Prestridge, Paul Rightley, Chris Tomkins, and Peter Vorobieff. Other technical contributors to the experiments are Jim Doyle, Cherie Goodenough, David Jenkins, David Klein, and Ryan Martin. Computational researchers who collaborated include Rose Mary Baltrusaitis, Mike Gittings, James Kamm, William Rider, Robert Weaver, and Cindy Zoldi. Technical editing and compositing were done by Deborah Magid.

References

1. P. Vorobieff et al., "Scaling Evolution in Shock-Induced Transition to Turbulence," to appear in *Physical Rev. E*, 2004.
2. C. Tomkins et al., "A Quantitative Study of the Interaction of Two Richtmyer-Meshkov-Unstable Gas Cylinders," *Physics of Fluids*, vol. 15, no. 4, 2003, pp. 986–1004.
3. C.A. Zoldi, *A Numerical and Experimental Study of a Shock-Accelerated Heavy Gas Cylinder*, doctoral thesis, Dept. of Applied Mathematics, State Univ. of New York at Stony Brook, 2002.
4. C. Tomkins et al., "Flow Morphologies of Two Shock-Accelerated Unstable Gas Cylinders," *J. Visualization*, vol. 5, no. 3, 2002, pp. 273–283.
5. K. Prestridge et al., "Validation of an Instability Growth Model Using Particle Image Velocimetry Measurements," *Physical Rev. Letters*, vol. 84, no. 19, 2000, pp. 4353–4356.
6. P.M. Rightley et al., "Experimental Observations of the Mixing Transition in a Shock-Accelerated Gas Curtain," *Physics of Fluids*, vol. 11, no. 1, 1999, pp. 186–200.
7. P. Vorobieff et al., "Shock-Driven Gas Curtain: Fractal Dimension

Evolution in Transition to Turbulence," *Physica D*, vol. 133, nos. 1–4, 1999, pp. 469–476.

8. P. Vorobieff, P.M. Rightley, and R.F. Benjamin, "Power-Law Spectra of Incipient Gas-Curtain Turbulence," *Physical Rev. Letters*, vol. 81, no. 11, 1998, pp. 2240–2243.
9. P.M. Rightley, P. Vorobieff, and R.F. Benjamin, "Evolution of a Shock-Accelerated Thin Fluid Layer," *Physics of Fluids*, vol. 9, no. 6, 1997, pp. 1770–1782.
10. R.M. Baltrusaitis et al., "Simulation of Shock-Generated Instabilities," *Physics of Fluids*, vol. 8, no. 9, 1996, pp. 2471–2483.
11. J.M. Budzinski and R.F. Benjamin, "Influence of Initial Conditions on the Flow Patterns of a Shock-Accelerated Thin Fluid Layer," *Physics of Fluids*, vol. 6, no. 11, 1994, pp. 3510–3512.
12. J.W. Jacobs et al., "Nonlinear Growth of the Shock-Accelerated Instability of Thin Fluid Layer," *J. Fluid Mechanics*, vol. 295, 25 July 1995, pp. 23–42.
13. J.W. Jacobs et al., "Instability Growth Patterns of a Shock-Accelerated Thin Fluid Layer," *Physical Rev. Letters*, vol. 70, no. 5, 1993, pp. 583–586.
14. W.L. Oberkampf and T.G. Trucano, "Validation Methodology in Computational Fluid Dynamics," *AIAA Fluids 2000 Conf.*, AIAA Paper 2000-2549, AIAA, 2000.
15. W.L. Oberkampf and T.G. Trucano, "Verification and Validation in Computational Fluid Dynamics," *Progress in Aerospace Sciences*, vol. 38, no. 3, 2002, pp. 209–272.
16. R.E. Reinovsky, "Pulsed Power Experiments in Hydrodynamics and Material Properties," *IEEE Trans. Plasma Science*, vol. 28, no. 5, 2000, pp. 1333–1337.
17. J.T. Waddell, C.E. Niederhaus, and J.W. Jacobs, "Experimental Study of Rayleigh-Taylor Instability: Low Atwood Number Liquid Systems with Single-Mode Initial Perturbations," *Physics of Fluids*, vol. 13, no. 5, 2001, pp. 1263–1273.
18. P. Ramaprabhu and M.J. Andrews, "Experimental Investigation of Rayleigh-Taylor Mixing at Small Atwood Numbers," submitted to *J. Fluid Mechanics*, Apr. 2003.
19. G. Dimonte et al., "A Linear Electric Motor to Study Turbulent Hydrodynamics," *Rev. Scientific Instruments*, vol. 67, no. 1, 1996, pp. 302–306.
20. N. Zabusky, "Vortex Paradigm for Accelerated Inhomogeneous Flows: Visiometrics for the Rayleigh-Taylor and Richtmyer-Meshkov Environments," *Ann. Rev. Fluid Mechanics*, vol. 31, 1999, pp. 495–535.
21. J.W. Jacobs, "The Dynamics of Shock Accelerated Light and Heavy Gas Cylinders," *Physics of Fluids A*, vol. 5, no. 9, 1993, pp. 2239–2247.
22. D.P. Aeschliman and W.L. Oberkampf, "Experimental Methodology for Computational Fluid Dynamics Code Validation," *AIAA J.*, vol. 36, no. 5, 1998, pp. 733–741.
23. M.L. Gittings, "SAIC's Adaptive Grid Eulerian Hydrocode," *Defense Nuclear Agency Numerical Methods Symp.*, 1992, pp. 28–30.
24. J. Kamm et al., "The Gas Curtain Experimental Technique and Analysis Methodologies," *Computational Methods and Experimental Measurements X, Y*, V. Esteve, G.M. Carlomagno, and C.A. Brebbia, eds., WIT Press, 2001.

Robert F. Benjamin is a Laboratory Fellow at the Los Alamos National Laboratory. His technical interests include fluid dynamics, inertial confinement fusion, explosively-driven pulse power, innovative sensors and diagnostics, and high-speed photography. He is the senior author of *Spills and Ripples*, the first book about fluid instability written for pre-college students. He has a BS in engineering physics from Cornell University and a PhD in physics from the Massachusetts Institute of Technology.